

## Super-Nernstian Shifts of Interfacial Proton-Coupled Electron Transfers: Origin and Effect of Non-Covalent Interactions

Christopher Wildi, Gema Cabello, Martin Eduardo Zoloff Michoff, Patricio Vélez Romero, Ezequiel Leiva, Juan Jose Calvente, Rafael Andreu, and Angel Cuesta

*J. Phys. Chem. C*, **Just Accepted Manuscript** • DOI: 10.1021/acs.jpcc.5b04560 • Publication Date (Web): 06 Jul 2015

Downloaded from <http://pubs.acs.org> on July 7, 2015

### Just Accepted

“Just Accepted” manuscripts have been peer-reviewed and accepted for publication. They are posted online prior to technical editing, formatting for publication and author proofing. The American Chemical Society provides “Just Accepted” as a free service to the research community to expedite the dissemination of scientific material as soon as possible after acceptance. “Just Accepted” manuscripts appear in full in PDF format accompanied by an HTML abstract. “Just Accepted” manuscripts have been fully peer reviewed, but should not be considered the official version of record. They are accessible to all readers and citable by the Digital Object Identifier (DOI®). “Just Accepted” is an optional service offered to authors. Therefore, the “Just Accepted” Web site may not include all articles that will be published in the journal. After a manuscript is technically edited and formatted, it will be removed from the “Just Accepted” Web site and published as an ASAP article. Note that technical editing may introduce minor changes to the manuscript text and/or graphics which could affect content, and all legal disclaimers and ethical guidelines that apply to the journal pertain. ACS cannot be held responsible for errors or consequences arising from the use of information contained in these “Just Accepted” manuscripts.



# Super-Nernstian Shifts of Interfacial Proton-Coupled Electron Transfers: Origin and Effect of Non- Covalent Interactions

*Christopher Wildi,<sup>†</sup> Gema Cabello,<sup>‡</sup> Martín E. Zoloff Michoff,<sup>§</sup> Patricio Vélez,<sup>#</sup> Ezequiel P. M. Leiva,<sup>#</sup> Juan José Calvente,<sup>⊥</sup> Rafael Andreu,<sup>⊥</sup> and Angel Cuesta<sup>\*†</sup>*

<sup>†</sup> Department of Chemistry, University of Aberdeen, Aberdeen AB24 3UE, UK

<sup>‡</sup> Department of Chemistry, Universidade Federal de São Carlos (UFSCAR), 13565-905, São Carlos, SP, Brazil

<sup>§</sup> Lehrstuhl für Theoretische Chemie, Ruhr-Universität Bochum, 44801 Bochum, Germany

<sup>#</sup> Facultad de Ciencias Químicas, Universidad Nacional de Córdoba, INFIQC, Córdoba, Argentina

<sup>⊥</sup> Departamento de Química Física, Universidad de Sevilla, 41012 Sevilla, Spain

**ABSTRACT:** Anions whose specific adsorption involves a proton-coupled electron transfer (PCET) include adsorbed OH ( $\text{OH}_{\text{ad}}$ ), which plays an enormously relevant role in many fuel-cell reactions.  $\text{OH}_{\text{ad}}$  formation has often been found to happen in alkaline solutions at potentials more negative than expected from a Nernstian shift, and this has been proposed as the reason for the

1  
2  
3 often easier oxidation of organic molecules in alkaline media, as compared to acids. Non-  
4  
5 covalent interactions with electrolyte cations have also been shown to affect the stability of  
6  
7  $\text{OH}_{\text{ad}}$ . Using cyanide-modified Pt(111) as a model, we show here that interfacial PCETs will  
8  
9 show a super-Nernstian shift if (i) less than one electron per proton is transferred, and (ii) the  
10  
11 plane of proton-electron transfer and that of the metal surface do not coincide. We also show that  
12  
13 electrolyte cations have a double effect: they provoke an additional shift by blocking the site of  
14  
15 transfer, but decrease the super-Nernstian contribution by separating the plane of transfer from  
16  
17 the outer Helmholtz plane (OHP).  
18  
19  
20  
21  
22

## 23 24 1. INTRODUCTION

25  
26  
27 All chemical reactions involve the transfer of either ions, electrons, or both. The most common  
28  
29 of the latter are proton-coupled electron transfers (PCET). Excluding that of coal, all the  
30  
31 combustion reactions on which modern energy-consuming economies are largely based involve  
32  
33 several PCETs. When performed electrochemically, the PCET steps of these reactions often  
34  
35 correspond to the formation on the electrode surface of H, OH, or O adlayers, or of surface  
36  
37 oxides, whose stability is crucial in determining the activity of the electrode as an electrocatalyst.  
38  
39 Since PCETs nominally involve the transfer of the same number of electrons and protons, the  
40  
41 equilibrium potential of any such reaction should always shift -0.059 V per pH unit. However, it  
42  
43 has been known for over three decades that the oxidation of metal surfaces in alkaline solutions  
44  
45 occurs at potentials more negative than expected from a purely Nernstian shift.<sup>1-3</sup> Although, as  
46  
47 far as we know, no satisfactory explanation for this has been yet given, this apparent stabilization  
48  
49 of surface oxygenated species with increasing pH beyond that expected from Nernst's equation  
50  
51  
52  
53  
54  
55  
56  
57  
58  
59  
60

1  
2  
3 can significantly affect the electrocatalytic activity of the electrode surface,<sup>4</sup> and the magnitude  
4  
5 of this effect has been found to be cation-dependent.<sup>5</sup>  
6  
7

8  
9 Very recently,<sup>6</sup> we have employed cyanide-modified Pt(111) electrodes (Pt(111) electrodes  
10  
11 chemically modified by spontaneous and irreversible adsorption of a cyanide adlayer,<sup>7,8</sup> which  
12  
13 have proven to be excellent model surfaces for the study of atomic-ensemble effects in  
14  
15 electrocatalysis<sup>9-13</sup>) to study the interaction between specifically adsorbed anions and alkali-  
16  
17 metal cations at electrode-electrolyte interfaces, and developed a simple model which we later  
18  
19 showed can be generalized to completely different systems.<sup>14</sup> Here, we use cyanide-modified  
20  
21 Pt(111) electrodes to offer an explanation for the occurrence of the above-mentioned super-  
22  
23 Nernstian shifts, as well as for the cation dependence of the magnitude of those shifts.  
24  
25  
26  
27

## 28 29 **2. EXPERIMENTAL**

30  
31  
32 Buffer solutions of pH 2, 4, 6, 8, 10 and 11 were prepared using H<sub>3</sub>PO<sub>4</sub> (Aldrich, 85% wt. in  
33  
34 H<sub>2</sub>O), NaH<sub>2</sub>PO<sub>4</sub> (Sigma-Aldrich, puriss. p.a., ≥ 99.0%), Na<sub>2</sub>HPO<sub>4</sub> (Sigma-Aldrich, puriss. p.a.,  
35  
36 98.5-101%), and Na<sub>3</sub>PO<sub>4</sub> (Sigma-Aldrich, puriss. p.a., ≥ 98.0%). When necessary, NaClO<sub>4</sub>  
37  
38 (Sigma-Aldrich for HPLC, ≥ 99.0%) was added to the buffer solutions in order to keep the  
39  
40 concentration of Na<sup>+</sup> and the ionic strength of the solution constant, and equal to 0.2 M. (See the  
41  
42 Supporting Information for exact composition of buffer solutions.)  
43  
44  
45  
46

47  
48 The pH values of the buffer solutions were accurately determined by measuring the open-circuit  
49  
50 potential of a platinum wire in a hydrogen-saturated buffer solution vs. a home-made Ag/AgCl  
51  
52 (KCl<sub>sat</sub>) reference electrode. The experiments examining the pH effect on the CV of cyanide-  
53  
54 modified Pt(111) electrodes were performed using this home-made Ag/AgCl (KCl<sub>sat</sub>) electrode  
55  
56 as reference, and the measured potentials were then converted either to the RHE or the SHE  
57  
58  
59  
60

1  
2  
3 scale. CO adlayers for the CO-stripping experiments were formed by bubbling CO through the  
4 solution at  $E_d = 0.1$  V, the solution being then purged with  $N_2$ . A home-made RHE was used as  
5 reference in the CO-stripping experiments. Other experimental details have been reported  
6  
7  
8  
9  
10 previously,<sup>8,9,12,13</sup> and can be found in the Supporting Information.

11  
12  
13 All calculations were performed using the DFT code SIESTA.<sup>15</sup> Exchange and correlation  
14 effects were taken into account using the generalized gradient approximation within the Perdew-  
15 Burke-Ernzerhof (PBE).<sup>16</sup> Norm-conserving pseudopotentials (with relativistic corrections in the  
16 case of Pt) generated according to the scheme of Troullier and Martins<sup>17,18</sup> were used. All  
17  
18  
19  
20  
21  
22  
23 calculations were performed with spin polarization and using a double-z basis set with  
24  
25  
26  
27 polarization and an energy shift, used to confine the electrons in the pseudopotentials, of 5 meV.  
28 For the energy cutoff that defines the fineness of the real space grid used to represent the charge  
29  
30  
31  
32  
33  
34  
35  
36  
37  
38  
39  
40  
41  
42  
43  
44  
45  
46  
47  
48  
49  
50  
51  
52  
53  
54  
55  
56  
57  
58  
59  
60  
Information.

### 3. RESULTS AND DISCUSSION

41  
42  
43  
44  
45  
46  
47  
48  
49  
50  
51  
52  
53  
54  
55  
56  
57  
58  
59  
60  
Fig. 1(A) shows the effect of increasing the pH on the cyclic voltammograms (CVs) of cyanide-  
modified Pt(111) electrodes. All the CVs show two distinct regions (appearing at  $E < 0.6$  V and  
at  $E > 0.8$  V at pH 1), attributed to hydrogen and OH adsorption, respectively,<sup>7,8,11,19</sup> separated  
by a double-layer region. Would hydrogen and OH adsorption shift -0.059 V per pH unit, as  
should be expected, they would appear at exactly the same potential in the reversible hydrogen  
electrode (RHE) scale used in Fig. 1(A), whatever the solution pH. However, both regions  
clearly shift negatively with increasing pH, the effect being larger in the case of the hydrogen

adsorption region. Hydrogen evolution, on the contrary, shows the expected Nernstian behavior, and occurs at the same potential on the RHE scale at all pHs studied.

We have recently identified the region appearing at  $E < 0.6$  V at pH 1 as a PCET to adsorbed CN ( $\text{CN}_{\text{ad}}$ ) to yield adsorbed CNH ( $\text{CNH}_{\text{ad}}$ ),<sup>20</sup> an idea already proposed by Schardt et al.<sup>21</sup> The exact nature of the adsorption process on cyanide-modified Pt(111) electrodes at  $E > 0.8$  V is still unknown, so we will concentrate our analysis on the hydrogen adsorption region.

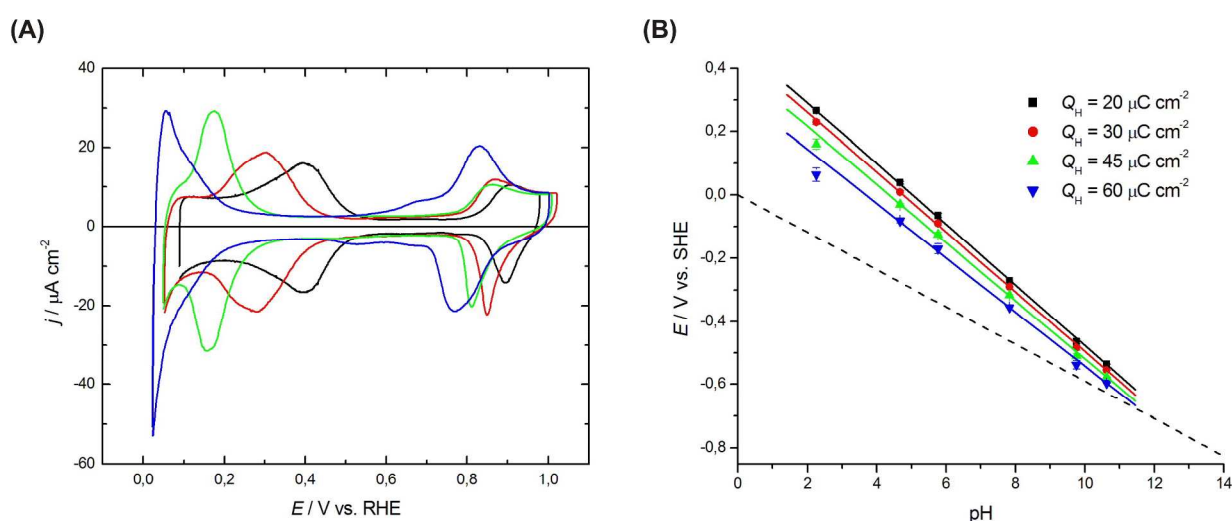


**Figure 1.** (A) Cyclic voltammograms at  $50 \text{ mV s}^{-1}$  of a cyanide-modified Pt(111) electrode in phosphate-buffer solutions of pH 2 (black line), 4 (red line), 8 (green line) and 11 (blue line). Adequate amounts of  $\text{NaClO}_4$  were added to the solutions in order to keep the ionic strength and the concentration of  $\text{Na}^+$  constant. (B) Potential (in the SHE scale) vs. pH at constant hydrogen-adsorption charge densities of  $20 \mu\text{C cm}^{-2}$  (black),  $30 \mu\text{C cm}^{-2}$  (red),  $45 \mu\text{C cm}^{-2}$  (green), and  $60 \mu\text{C cm}^{-2}$  (blue). For the sake of comparison a line with a slope of  $-0.059 \text{ V}$ , corresponding to the Nernstian behaviour expected for a PCET has also been included (dashed line).

1  
2  
3 Metal cations in the electrolyte can interact with the nitrogen atoms of  $\text{CN}_{\text{ad}}$ , thus blocking the  
4 sites where the PCET occurs,<sup>6,20</sup> and increasing the concentration of alkali-metal cations above a  
5 cation-dependent threshold concentration provokes a negative shift of the onset of hydrogen  
6 adsorption on cyanide-modified Pt(111) electrodes.<sup>6</sup> However, in the experiments reported in  
7 Fig. 1 we paid particular attention to keeping the ionic strength and the  $\text{Na}^+$  concentration  
8 constant (see Supporting Information), so we can exclude any variable other than pH as the cause  
9 of the shift. The total charge density in the hydrogen adsorption region remains constant, within  
10 experimental error, at  $\text{pH} \leq 8$  (i.e., within this pH range, the maximum  $\text{CNH}_{\text{ad}}$  coverage ( $\theta_{\text{CNH}}$ )  
11 achievable is pH-independent). At the highest pHs studied (10 and 11) it decreases slowly,  
12 because hydrogen evolution starts before the maximum  $\theta_{\text{CNH}}$  has been attained.  
13  
14  
15  
16  
17  
18  
19  
20  
21  
22  
23  
24  
25  
26  
27

28 Figure 1(B) shows plots of the potential (vs. the standard hydrogen electrode, SHE) at constant  
29 charge density (i.e., at constant  $\theta_{\text{CNH}}$ ) vs. pH. A line with a slope of -0.059 V has been included  
30 as a guide to the eye. At all coverages, the potential shift is larger than the -0.059 V per pH unit  
31 expected for a PCET. The super-Nernstian contribution decreases slightly as  $\theta_{\text{CNH}}$  approaches the  
32 maximum coverage possible (see Table S2), but at all  $\theta_{\text{CNH}}$  the shift of the equilibrium potential  
33 with pH remains far from the expected Nernstian value.  
34  
35  
36  
37  
38  
39  
40  
41  
42  
43

44 Hydrogenation of  $\text{CN}_{\text{ad}}$  on cyanide-modified Pt(111) is a very reversible process, as reflected by  
45 the symmetric shape of the CV in the corresponding potential region, even at high scanning  
46 rates. Accordingly, every potential within the hydrogen adsorption region corresponds to a well-  
47 defined equilibrium, i.e., when measured vs. the RHE, the potential at which a given  $\theta_{\text{CNH}}$  is  
48 reached corresponds to  $-\Delta G$  at 0 V vs. RHE for the hydrogenation of  $\text{CN}_{\text{ad}}$  up to that  $\theta_{\text{CNH}}$  (at the  
49 potential at which a given equilibrium  $\theta_{\text{CNH}}$  is reached,  $\Delta G$  for the hydrogenation of  $\text{CN}_{\text{ad}}$  up to  
50  
51  
52  
53  
54  
55  
56  
57  
58  
59  
60

that  $\theta_{\text{CNH}}$  is obviously zero).  $\Delta G$  only depends on the initial ( $\text{CN}_{\text{ad}} + \text{H}^+ + e$ ) and the final ( $\text{CNH}_{\text{ad}}$ ) states of the reaction. The Nernstian shift accounts for the decrease in the chemical potential of  $\text{H}^+$  as the pH increases. A super-Nernstian shift of the equilibrium potential for a given  $\theta_{\text{CNH}}$  suggests, hence, an additional stabilization of the initial state and/or an additional destabilization of the final state with increasing pH, by an amount identical to the super-Nernstian contribution.

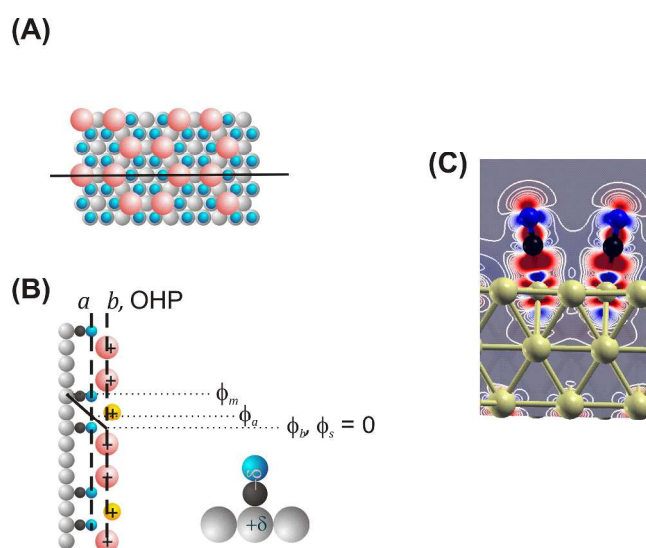


**Figure 2.** (A) Ball model of the structure of cyanide-modified Pt(111), with cations (red balls) interacting non-covalently with  $\text{CN}_{\text{ad}}$  (blue balls) forming the experimentally observed honeycomb structure.<sup>6</sup> Grey balls correspond to the substrate Pt atoms. (B) Cross section along the solid line in (A), and schematic representation of the electrical double layer, indicating the location of the plane of proton-electron transfer,  $a$ , and of the plane of maximum approach of cations and protons,  $b$  (which, for the sake of simplicity, we have made coincide with the OHP, see text). Black balls correspond to the carbon atoms, and blue balls to the nitrogen atoms, respectively, of the CN groups. Yellow balls correspond to hydrated protons. The inset illustrates the polar nature of the chemisorption bond. (C) Electronic density difference with respect to the

1  
2  
3 separated fragments, CN and Pt slab, represented on a plane that cuts through the Pt-CN bond.  
4  
5 The separation between contiguous isocurves is  $7.5 \times 10^{-4}$  electrons / Bohr<sup>3</sup>, ranging from -  
6  
7 0.0075 in blue to +0.0075 in red. N atoms are blue, C atoms are black, and Pt atoms are light  
8  
9 yellow.  
10

11  
12  
13 Fig. 2(A) shows a ball model of the structure of the cyanide-modified Pt(111) surface with  
14  
15 cations adsorbed at sites surrounded by 3 CNs, as in the experimentally observed honeycomb  
16  
17 structure.<sup>6</sup> Fig. 2(B) shows a cross section along the line in Fig. 2(A), and a schematic  
18  
19 representation of the electrode-electrolyte interface. The PCET will occur at plane *a*, defined by  
20  
21 the position of the specifically adsorbed hydrogen acceptor/proton donor, namely, the N atom of  
22  
23 CN<sub>ad</sub>/CNH<sub>ad</sub>. The presence of the cations interacting non-covalently with CN<sub>ad</sub> defines a plane of  
24  
25 maximum approach *b*, where the proton donor (H<sub>3</sub>O<sup>+</sup> in acidic solutions, H<sub>2</sub>O in alkaline  
26  
27 solutions) or acceptor (H<sub>2</sub>O in acidic solutions, OH<sup>-</sup> in alkaline solutions) has to be transferred  
28  
29 from the limit of the diffuse double layer (which, in concentrated solutions as the ones used here  
30  
31 will coincide with the outer Helmholtz plane, OHP), before reaching *a* for the PCET to occur. In  
32  
33 other words, protons have to displace the cations from this plane, and this explains the recently  
34  
35 reported effect of increasing the cation concentration at constant pH on the hydrogen adsorption  
36  
37 region of cyanide-modified Pt(111) electrodes.<sup>6</sup>  
38  
39  
40  
41  
42  
43  
44

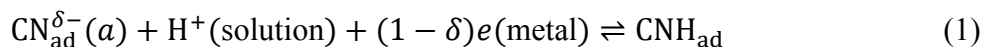
45 **Table 1.** Hirshfeld and Voronoi atomic charge analysis CN<sub>ad</sub> on Pt(111) in the experimentally  
46  
47 observed ( $2\sqrt{3} \times 2\sqrt{3}$ )R30° structure (see Fig. 3A).  
48  
49

Atoms	Atomic charges / <i>e</i>	
	Hirshfeld	Voronoi
C	-0.20	-0.278

N	-0.14	-0.11
Pt(C) <sup>[a]</sup>	+0.19	+0.22
Pt, 1 <sup>st</sup> layer average <sup>[b]</sup>	+0.16	+0.18
Pt, 2 <sup>nd</sup> layer average <sup>[c]</sup>	+0.02	+0.03
Pt, 3 <sup>rd</sup> layer average <sup>[d]</sup>	-0.01	-0.02

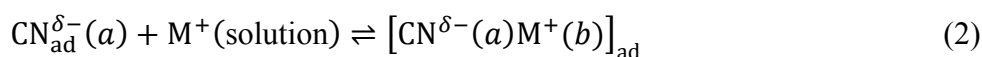
[a] Atomic charge for the Pt atom directly bounded to the adsorbed CN. The value reported is an average of all 6 equivalent positions. [b] Average value for all the atoms in the 1<sup>st</sup> layer with respect to the adsorbate. [c] Average value for all the atoms in the 2<sup>nd</sup> layer with respect to the adsorbate. [d] Average value for all the atoms in the 3<sup>rd</sup> layer with respect to the adsorbate.

The hydrogenation of adsorbed cyanide can be described as:



where  $0 \leq \delta \leq 1$  corresponds to the residual charge on adsorbed cyanide, and is related to the polar nature of the M-CN<sub>ad</sub> chemisorption bond (for an excellent discussion about specific adsorption and partial charge transfer, please see the recent review by Schmickler and Guidelli<sup>22</sup>). The polar nature of the M-CN<sub>ad</sub> bond is supported by DFT calculations of the electronic density difference of the separated fragments, CN and Pt surface (Figure 2(C)), and of atomic charge analysis of the adsorbate (Table 1). Actually, the M-CN<sub>ad</sub> bond will also certainly be polar, but the relevant magnitude here is the change in the dipole moment of the adsorbed species as a consequence of the proton-electron transfer, which transforms CN<sub>ad</sub> into CNH<sub>ad</sub>. Considering nil dipole moment after the PCET (as we have done in Reaction 1, to keep the argument as simple as possible), nil dipole moment before the PCET, or a finite dipole moment both before and after the PCET, is irrelevant, because only the difference counts.

The fraction of the cyanide adlayer corresponding to  $\text{CNH}_{\text{ad}}$  is given by  $\theta_{\text{CNH}} = \frac{Q_{\text{H}}}{(1-\delta)F\Gamma_{\text{T}}}$ , where  $\Gamma_{\text{T}}$  is the total number of moles ( $\text{CN}_{\text{ad}} + \text{CNH}_{\text{ad}}$ ) per unit area, and  $Q_{\text{H}}$  is the charge (double-layer corrected) obtained by integrating the CV between the double layer and a given potential within the hydrogen adsorption region. In the presence of a metal cation  $\text{M}^+$  in the solution, a fraction  $\theta_{\text{CNM}} = 1 - \theta_{\text{CN}} - \theta_{\text{CNH}}$  of the cyanide adlayer (where  $\theta_{\text{CN}}$  is the fraction of adsorbed cyanide that remains available for hydrogenation) will be blocked by cations interacting non-covalently with the nitrogen atoms of  $\text{CN}_{\text{ad}}$ .<sup>6</sup> Non-reductive adsorption of  $\text{M}^+$  on the metal surface through non-covalent interactions with  $\text{CN}_{\text{ad}}$  can be described as:



Assuming that the potential drop across the interface is linear, the potential drop between plane  $i$  and the solution,  $\phi^i$ , will be a fraction of the total potential drop across the interface,  $\phi^m$ , given by:

$$\phi^i = \omega_i \phi^m \quad (3)$$

where  $\omega_i = C_{m/\text{OHP}}/C_{i/\text{OHP}}$ , with  $C_{m/\text{OHP}}$  the integral capacity of the electrical double layer, and  $C_{i/\text{OHP}}$  the integral capacity of a dielectric slab limited by plane  $i$  and the OHP (i.e.,  $0 \leq \omega_i \leq 1$ ;  $\omega_b \leq \omega_a$ ). The condition under which both reactions (1) and (2) are in equilibrium is:

$$\phi^m = f(\theta_{\text{CNH}}) + \frac{RT}{[1-\delta(1-\omega_a)]F} \ln \frac{a_{\text{H}^+}}{1 + K_{\text{as}} \exp\left(\frac{-\omega_b F \phi^m}{RT}\right) a_{\text{M}^+}} \quad (4)$$

with  $f(\theta_{\text{CNH}}) = \frac{RT}{[1-\delta(1-\omega_a)]F} \left( \frac{-\Delta G_{\text{H}^+/\text{H}}^0}{RT} + \ln \frac{1-\theta_{\text{CNH}}}{\theta_{\text{CNH}}} \right)$ , where  $-\Delta G_{\text{H}^+/\text{H}}^0 = \mu_{\text{CN}}^0 + \mu_{\text{H}^+}^0 +$

$(1-\delta)\mu_e^0 - \mu_{\text{CNH}}^0$ .  $\phi^m$  is the electrode's Galvani potential referred to that of the solution,  $a_{\text{H}^+}$  is

the activity of  $H^+$  in the bulk solution,  $K_{as} = \exp(-\Delta G_{as}^0/RT)$  is the association constant of the non-reductive adsorption of  $M^+$  on the cyanide adlayer at  $\phi^m = 0$  (with  $-\Delta G_{as}^0 = \mu_{CN}^0 + \mu_{M^+}^0 - \mu_{CNM}^0$ ), and  $a_{M^+}$  is the activity of  $M^+$  in the bulk solution. The rest of the terms have their usual meaning. (For a complete deduction of Equation (4) please see the Supporting Information.)

If plane  $b$  is close enough to the OHP (i.e.,  $\omega_b \rightarrow 0$ ), as assumed in Fig. 2(B), Equation (4) simplifies to:

$$\phi^m = f(\theta_{CNH}) + \frac{RT}{[1-\delta(1-\omega_a)]F} \ln \frac{a_{H^+}}{1+K_{as}a_{M^+}} \quad (5)$$

Equations (4) and (5) are generalizations of the expression recently derived for proton transfer to acid thiol monolayers,<sup>23</sup> in which the possibility of an electron transfer coupled to the proton transfer, as well as that of another cation competing with  $H^+$  for the proton acceptor, have been taken into account.

Equation (5) predicts that a super-Nernstian shift will happen only whenever  $\delta \neq 0$  and  $\omega_a \neq 1$  ( $\omega_a = 1$  when plane  $a$  is infinitely closer to the metal surface than to the OHP, while  $\omega_a = 0$  when plane  $a$  is infinitely closer to the OHP than to the metal surface). This condition implies that (i) less than one electron per proton is transferred to the proton acceptor, and (ii) the separation between plane  $a$  and the OHP is comparable to that between the metal surface and plane  $a$ . This agrees with the fact that hydrogen evolution shows the expected Nernstian behavior (see Fig. 1(A)). In the case of a pure proton transfer ( $\delta = 1$ ) taking place at the OHP ( $\omega_a = 0$ ), the protonation degree of the adlayer depends only on the pH of the solution, and is not affected by the electrode potential.

Fig. 3(A) shows level curves indicating the combinations of values of  $\delta$  and  $\omega_a$  for which the shift with pH of the equilibrium potential of the PCET up to a given  $\theta_{\text{CNH}}$  would have slopes of -0.061 (black), -0.070 (red), -0.080 (green), -0.090 (blue), and -0.100 V (cyan). Although a true Nernstian behaviour will only occur if  $\delta = 0$ , whatever the value of  $\omega_a$ , or if  $\omega_a = 1$ , whatever the value of  $\delta$ , the shaded area in Fig. 3 shows that the range of combinations of  $\delta$  and  $\omega_a$  for which the slope would be between -0.059 and -0.061 V (i.e., for which the difference between Nernstian behaviour and the actual one would be too small to be detected experimentally) is relatively large.

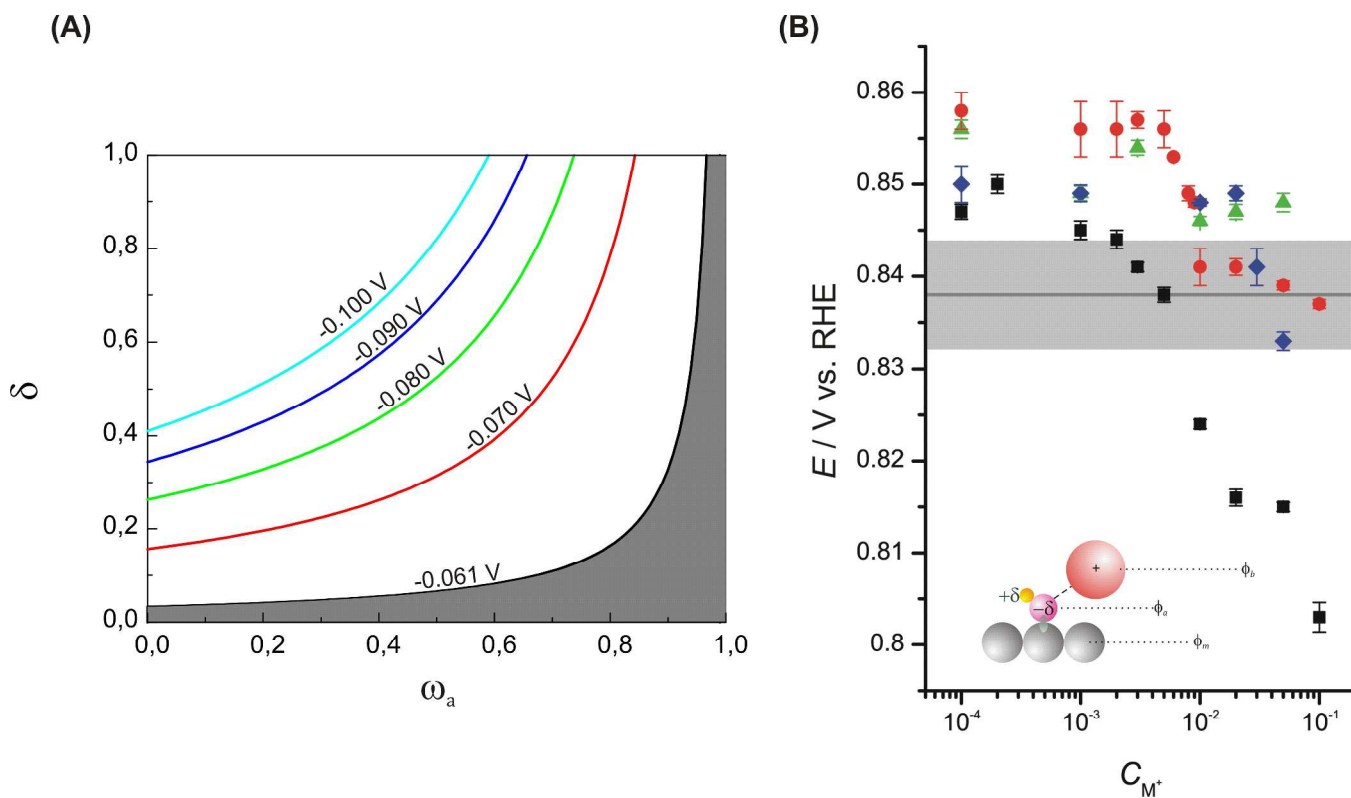


**Figure 3.** (A) Level curves indicating the possible combinations of  $\delta$  and  $\omega_a$  for selected values of the slope of a plot vs. the pH of the equilibrium potential of the PCET to  $\text{CN}_{\text{ad}}$  on cyanide-modified Pt(111) electrodes up to a given  $\theta_{\text{CNH}}$ . For  $\delta = 0$  and for  $\omega_a = 1$ , the slope would be -0.059 V, whatever the value of  $\omega_a$  and  $\delta$ , respectively. The grey shaded area corresponds to all

the possible combinations of  $\delta$  and  $\omega_a$  for which the slope will be between -0.059 and -0.061 V, i.e., for which the difference between a Nernstian behaviour and the actual one will be too small to be detected experimentally. **(B)** Semilogarithmic plot of the dependence on the concentration of alkaline-metal cations of the peak in CO-stripping voltammograms of Pt(111) in 0.1 M H<sub>2</sub>SO<sub>4</sub> at 50 mV s<sup>-1</sup>. (black squares: Li<sup>+</sup>; red circles: Na<sup>+</sup>; green triangles: K<sup>+</sup>; blue rhombi: Cs<sup>+</sup>). The horizontal line marks the average potential of the CO-stripping peak in alkaline-cations-free 0.1 M H<sub>2</sub>SO<sub>4</sub>, and the grey-shaded area indicates the corresponding standard deviation. The inset shows a schematic representation of the electrical double layer, with electrolyte cations interacting non-covalently with OH<sub>ad</sub> (grey balls: metal surface; pink ball: oxygen; yellow ball: hydrogen; red ball: alkaline-metal cation).

It is interesting to analyse two possible kinds of experiments:

1. The cation concentration is kept constant and the pH is changed, as in Fig. 1. Under these conditions, Equation (5) becomes:

$$\phi^m = f'(\theta_{\text{CNH}}) + \frac{RT}{[1-\delta(1-\omega_a)]F} \ln a_{\text{H}^+} \quad (6)$$

$$\text{with } f'(\theta_{\text{CNH}}) = \frac{RT}{[1-\delta(1-\omega_a)]F} \left( \frac{-\Delta G_{\text{H}^+/\text{H}}^0}{RT} + \ln \frac{1-\theta_{\text{CNH}}}{\theta_{\text{CNH}}} - \ln(1 + K_{\text{as}} a_{\text{M}^+}) \right).$$

Cations have an effect only above a  $K_{\text{as}}$ -dependent threshold concentration, such that

$$K_{\text{M}^+} a_{\text{M}^+}^S \gg 1. \text{ When } K_{\text{M}^+} a_{\text{M}^+}^S \ll 1, f'(\theta_{\text{CNH}}) = f(\theta_{\text{CNH}}) = \frac{RT}{[1-\delta(1-\omega_a)]F} \left( \frac{-\Delta G_{\text{H}^+/\text{H}}^0}{RT} + \ln \frac{1-\theta_{\text{CNH}}}{\theta_{\text{CNH}}} \right),$$

the cation layer interacting with CN<sub>ad</sub> does not exist, and plane  $a$  can be assumed to coincide with the OHP (i.e.,  $\omega_a \rightarrow 0$ ). Any super-Nernstian contribution is

1  
2  
3 due exclusively to the polar nature of the chemisorption bond between  $\text{CN}_{\text{ad}}$  and the  
4 metal surface. Above the threshold concentration, the presence of the cation layer (i)  
5 shifts  $f'(\theta_{\text{CNH}})$  negatively by  $\frac{RT}{[1-\delta(1-\omega_a)]F} \ln(1 + K_{as}a_{\text{M}^+})$  V (*i.e.*, even if  $\delta = 0$ , the  
6 PCET in MOH solutions will shift by  $-\frac{RT}{F} \ln(1 + K_{as}a_{\text{M}^+})$  V in the RHE, when  
7 compared to  $\text{HClO}_4$  or  $\text{H}_2\text{SO}_4$  solutions), and (ii) separates plane  $a$  from the OHP,  
8 making  $\omega_a \neq 0$  and decreasing the slope of the pH dependence (see Fig. 3(A)).  
9  
10  
11  
12  
13  
14  
15  
16  
17  
18  
19

- 20 2. The pH is kept constant and the cation concentration varies, as in reference [4]. Under  
21 these conditions, Equation (5) becomes:  
22  
23  
24

$$25 \quad \phi^m = f'(\theta_{\text{CNH}}) - \frac{RT}{[1-\delta(1-\omega_a)]F} \ln(1 + K_{as}a_{\text{M}^+}) \quad (7)$$

$$26 \quad \text{with } f'(\theta_{\text{CNH}}) = \frac{RT}{[1-\delta(1-\omega_a)]F} \left( \frac{-\Delta G_{\text{H}^+/\text{H}}^0}{RT} + \ln \frac{1-\theta_{\text{CNH}}}{\theta_{\text{CNH}}} + \ln a_{\text{H}^+} \right).$$

27  
28  
29  
30  
31  
32  
33  
34  
35 Equation (7) is equivalent to Equation 2 in ref. <sup>6</sup>. The equilibrium potential remains  
36 constant when  $K_{\text{M}^+}a_{\text{M}^+}^s \ll 1$ , and decreases logarithmically with increasing  $a_{\text{M}^+}^s$  when  
37  $K_{\text{M}^+}a_{\text{M}^+}^s \gg 1$ , as found in <sup>6</sup>. Cations for which plane  $b$  is located closer to plane  $a$  will  
38 show a larger non-Nernstian contribution (smaller  $\omega_a$ ) in the region of logarithmic  
39 dependence. This is in agreement with our previous results,<sup>6</sup> where we found the slope in  
40 the logarithmic dependence region to decrease according to the sequence  $\text{Li}^+ > \text{Na}^+ >$   
41  $\text{Cs}^+$ , as expected from their ionic radius.  $\text{K}^+$  deviates from this trend, most likely due to  
42 the excellent match between its ionic radius and the size of the  $(\text{CN}_{\text{ad}})_3$  cavity, which also  
43 provokes a deviation of its  $K_{as}$  from the expected trend, as discussed in reference [4].  
44  
45  
46  
47  
48  
49  
50  
51  
52  
53  
54  
55  
56  
57  
58  
59  
60

1  
2  
3 Equations (6) and (7) predict that, once the threshold concentration for a given  $M^+$  is reached, the  
4 slope of these two experiments must be identical. For  $M^+ = Na^+$ , and for a hydrogen adsorption  
5 charge of  $20 \mu C cm^{-2}$ , the experiments reported here yield  $z = 1 - \delta(1 - \omega_a) = 0.61$ , in perfect  
6 agreement with the value obtained in reference [4].  
7  
8  
9  
10  
11

12  
13  
14 The relevance of the discussion above is that it can be generalised for any PCET to any anion  
15 specifically adsorbed on an electrode surface, including  $OH_{ad}$  (see inset in Fig. 3(B)) or  $O_{ad}$ .  
16  
17 These species play an essential role in many fuel-cell reactions, like, e.g., the electrooxidation of  
18 CO, the methanol oxidation reaction (MOR), or the oxygen reduction reaction (ORR), where  
19 they provide the oxygen atom necessary for the formation of  $CO_2$  (CO electrooxidation, MOR),  
20 or can act as a catalytic poison (ORR). In alkaline solutions, the formation of surface oxygenated  
21 species often occurs at potentials more negative than expected from a merely Nernstian shift,<sup>1,2</sup>  
22 and this has been suggested to be the reason for the higher electrocatalytic activity of Pt and  
23 other metals in alkaline media towards the oxidation of some organic molecules, as compared to  
24 acidic environments.<sup>24-27</sup> Our work provides an explanation for these phenomena.  
25  
26  
27  
28  
29  
30  
31  
32  
33  
34  
35  
36  
37  
38

39 Furthermore, the presence of different alkaline and alkaline-earth metal cations has been shown  
40 to affect the activity of Pt towards several fuel-cell reactions, both in alkaline<sup>5,28-30</sup> and in acidic  
41 solutions.<sup>31</sup> Strmcnik et al.<sup>5</sup> qualitatively attributed this effect to the stabilisation of  $OH_{ad}$  via  
42 non-covalent interactions between the adsorbate and the cations, and the differences between  
43 cations to the cation-dependent strength of these interactions. Our model suggests that this  
44 apparent stabilisation of  $OH_{ad}$  is due to the energy required to remove the cations from plane *b*.  
45  
46 Moreover, our model additionally predicts that the cation effect will only be observed above a  
47 threshold concentration, and that the magnitude of the shift of OH adsorption with increasing pH  
48 or cation concentration will be different for different cations.  
49  
50  
51  
52  
53  
54  
55  
56  
57  
58  
59  
60

1  
2  
3 In order to confirm that our model can be generalised to the formation of  $\text{OH}_{\text{ad}}$  and  $\text{O}_{\text{ad}}$ , and,  
4 consequently, to the fuel-cell reactions in which they are involved, we studied the effect of the  
5 concentration of alkaline-metal cations on the electrooxidation of adsorbed CO (an archetypal  
6 electrocatalytic reaction) in 0.1 M  $\text{H}_2\text{SO}_4$ . The results for  $\text{Li}^+$ ,  $\text{Na}^+$ ,  $\text{K}^+$  and  $\text{Cs}^+$  are shown in Fig.  
7 3(B) (the corresponding CO-stripping voltammograms are shown in Fig. S2). In all the cases,  
8 addition of an alkaline-metal cation at so low a concentration as  $10^{-4}$  M provokes a positive shift  
9 of the CO-stripping peak potential, although this shift does not show any clear trend.

10 Interestingly, the reproducibility of the CO-stripping voltammogram is clearly higher at  $c_{\text{M}} \geq 10^{-4}$   
11 M than at lower, or nil, concentrations of alkaline-metal cations. It has been shown that a slight  
12 increase in the amount of defect sites on a Pt(111) electrode, too small to be detected in its CV in  
13 sulphuric acid solutions, can provoke a significant decrease in the CO-stripping peak potential.<sup>32</sup>  
14 Accordingly, we attribute the small positive shift, and the higher reproducibility, of the CO-  
15 stripping peak potential at  $c_{\text{M}} \geq 10^{-4}$  M to the preferential adsorption of  $\text{MSO}_4^-$  pairs<sup>14</sup> at defect  
16 sites, which are thus blocked as ignition sites for the CO-stripping reaction.

17 In all cases, increasing the cation concentration above a cation-dependent threshold provokes a  
18 negative shift of the CO-stripping peak potential. The minimum concentration at which the  
19 alkaline-metal cations start provoking a shift follows the trend:  $\text{Li}^+ < \text{Na}^+ \approx \text{K}^+ < \text{Cs}^+$ , in good  
20 agreement with the effect of the alkaline-metal cations on the CO-stripping voltammogram of  
21 Pt(100) in alkaline solutions,<sup>33</sup> and with the effect of the alkaline-metal cations on OH adsorption  
22 on Pt(111) in alkaline media.<sup>5</sup> This trend can be related to the corresponding trend in the  
23 association constant,  $K_{\text{as}}$ , of our model ( $\text{Li}^+ > \text{Na}^+ \approx \text{K}^+ > \text{Cs}^+$ ), i.e., with the strength of the  
24 interaction between the cation and  $\text{OH}_{\text{ad}}$ . The analysis of the slope in the region where the peak  
25 potential shows a dependence on the cation concentration is not straightforward, because in this  
26  
27  
28  
29  
30  
31  
32  
33  
34  
35  
36  
37  
38  
39  
40  
41  
42  
43  
44  
45  
46  
47  
48  
49  
50  
51  
52  
53  
54  
55  
56  
57  
58  
59  
60

1  
2  
3 case the peak potential does not correspond to an equilibrium situation. Furthermore, sulfate and  
4  
5 OH will compete for the adsorption sites left free during CO stripping and, since the cations also  
6  
7 affect the adsorption of sulfate,<sup>14</sup>  $\theta_{\text{OH}}$  at the peak will not necessarily be always the same, and  
8  
9 independent of the cation concentration. In spite of this, it is obvious that, as predicted by our  
10  
11 model, the shift of the voltammetric peak with increasing cation concentration is different for  
12  
13 different cations. Within the frame of our model, this is due to the creation, by the cations  
14  
15 interacting non-covalently with  $\text{OH}_{\text{ad}}$ , of a plane of maximum approach that separates the plane  
16  
17 where the proton-electron transfer occurs from the OHP, the location of this plane being cation-  
18  
19 dependent.  
20  
21  
22  
23  
24

#### 25 26 4. CONCLUSIONS

27  
28  
29 In summary, we have shown that PCETs to specifically adsorbed anions will show a super-  
30  
31 Nernstian shift with pH if the chemisorption bond is polar, and if the plane where the proton-  
32  
33 electron transfer occurs does not coincide with the electrode surface. These PCETs include OH  
34  
35 adsorption/desorption (which can be considered as the dehydrogenation/hydrogenation of  
36  
37  $(\text{H}_2\text{O})_{\text{ad}}/\text{OH}_{\text{ad}}$ ), and has therefore profound implications in fuel-cells electrocatalysis. Among  
38  
39 them, the frequently easier electrooxidation of organic fuels in alkaline as compared to acidic  
40  
41 media, for which our model provides an explanation. Above a cation-dependent threshold  
42  
43 concentration, the presence in the electrolyte of cations (other than  $\text{H}^+$ ) which can interact non-  
44  
45 covalently with specifically adsorbed anions, including  $\text{OH}_{\text{ad}}$ , has a double effect:  
46  
47  
48  
49

- 50  
51 (i) They will provoke an additional negative shift of the PCET, due to the energy  
52  
53 required to remove the cation layer before the proton can access the plane where the  
54  
55 hydrogenation occurs. This can be viewed as a purely thermodynamic effect, which  
56  
57  
58  
59  
60

1  
2  
3 increases the apparent adsorption energy of the dehydrogenated form of the  
4 specifically adsorbed species ( $CN_{ad}$ ,  $OH_{ad}$ ...). This effect was the only one taken into  
5  
6 account in previous interpretations of the effect of non-covalent interactions on  
7  
8 electrocatalytic reactions.<sup>5</sup>  
9  
10

- 11  
12  
13  
14 (ii) They will affect the magnitude of the super-Nernstian shift, by separating the plane of  
15  
16 hydrogenation and the OHP. This can be viewed as a double-layer effect that  
17  
18 counteracts the one above, and whose relevance had not be considered in previous  
19  
20 work.<sup>5</sup>  
21  
22

23  
24 As has been shown repeatedly,<sup>5,28-31</sup> these two effects can be used to tune the catalytic activity of  
25  
26 electrode-electrolyte interfaces.  
27  
28

## 29 30 ASSOCIATED CONTENT

31  
32  
33 Experimental details and computational methodology. Full deduction of Equation (4). This  
34  
35 material is available free of charge via the Internet at <http://pubs.acs.org>.  
36  
37

## 38 39 AUTHOR INFORMATION

40  
41  
42 **Corresponding Author:** \*E-mail: [angel.cuestaciscar@abdn.ac.uk](mailto:angel.cuestaciscar@abdn.ac.uk). Tel: +44 (0)1224 274538  
43  
44

## 45 46 ACKNOWLEDGMENT

47  
48 The support of the University of Aberdeen is gratefully acknowledged. CW acknowledges a  
49  
50 summer studentship from the Carnegie Trust for the Universities of Scotland. EPML  
51  
52 acknowledges SeCYT (Universidad Nacional de Córdoba), CONICET- PIP 11220110100992,  
53  
54 Program BID (PICT 2012-2324) and PME 2006-01581 for financial support.  
55  
56

## 57 58 REFERENCES

59  
60

- 1  
2  
3 (1) Burke, L. D.; Lyons, M. E.; Whelan, D. P. Influence of pH on the Reduction of Thick  
4 Anodic Oxide Films on Gold. *J. Electroanal. Chem.* **1982**, *139*, 131-142.
- 5  
6 (2) Burke, L. D.; Roche, M. B. C. The Possible Importance of Hydrolysis Effects in the Early  
7 Stages of Metal Surface Electrooxidation Reactions — With Particular Reference to Platinum. *J.*  
8 *Electroanal. Chem.* **1983**, *159*, 89-99.
- 9  
10 (3) Liu, C.; Bocchicchio, D.; Overmyer, P.; Neuman, M. A Palladium-Palladium Oxide  
11 Miniature pH Electrode. *Science* **1980**, *207*, 188-189.
- 12  
13 (4) Marković, N. M.; Schmidt, T. J.; Grgur, B. N.; Gasteiger, H. A.; Behm, R. J.; Ross, P. N.  
14 Effect of Temperature on Surface Processes at the Pt(111)–Liquid Interface: Hydrogen  
15 Adsorption, Oxide Formation, and CO Oxidation. *J. Phys. Chem. B* **1999**, *103*, 8568-8577.
- 16  
17 (5) Strmcnik, D.; Kodama, K.; van der Vliet, D.; Greeley, J.; Stamenkovic, V. R.; Marković,  
18 N. M. The Role of Non-Covalent Interactions in Electrocatalytic Fuel-Cell Reactions on  
19 Platinum. *Nat. Chem.* **2009**, *1*, 466-472.
- 20  
21 (6) Escudero-Escribano, M.; Zoloff Michoff, M. E.; Leiva, E. P. M.; Marković, N. M.;  
22 Gutiérrez, C.; Cuesta, Á. Quantitative Study of Non-Covalent Interactions at the Electrode–  
23 Electrolyte Interface Using Cyanide-Modified Pt(111) Electrodes. *ChemPhysChem* **2011**, *12*,  
24 2230-2234.
- 25  
26 (7) Huerta, F.; Morallón, E.; Quijada, C.; Vázquez, J. L.; Aldaz, A. Spectroelectrochemical  
27 Study on CN<sup>-</sup> Adsorbed at Pt(111) in Sulphuric and Perchloric Media. *Electrochim. Acta* **1998**,  
28 *44*, 943-948.
- 29  
30 (8) Morales-Moreno, I.; Cuesta, A.; Gutiérrez, C. Accurate Determination of the CO  
31 Coverage at Saturation on a Cyanide-Modified Pt(111) Electrode in Cyanide-Free 0.5 M H<sub>2</sub>SO<sub>4</sub>.  
32 *J. Electroanal. Chem.* **2003**, *560*, 135-141.
- 33  
34 (9) Cuesta, A. At Least Three Contiguous Atoms Are Necessary for CO Formation during  
35 Methanol Electrooxidation on Platinum. *J. Am. Chem. Soc.* **2006**, *128*, 13332-13333.
- 36  
37 (10) Cuesta, A. Atomic Ensemble Effects in Electrocatalysis: The Site-Knockout Strategy.  
38 *ChemPhysChem* **2011**, *12*, 2375-2385.
- 39  
40 (11) Strmcnik, D.; Escudero-Escribano, M.; Kodama, K.; Stamenkovic, V. R.; Cuesta, A.;  
41 Marković, N. M. Enhanced Electrocatalysis of the Oxygen Reduction Reaction Based on  
42 Patterning of Platinum Surfaces with Cyanide. *Nat. Chem.* **2010**, *2*, 880-885.
- 43  
44 (12) Cuesta, A.; Escudero, M. Electrochemical and FTIRS Characterisation of NO Adlayers  
45 on Cyanide-Modified Pt(111) Electrodes: the Mechanism of Nitric Oxide Electroreduction on Pt.  
46 *Phys. Chem. Chem. Phys.* **2008**, *10*, 3628-3634.
- 47  
48 (13) Cuesta, A.; Escudero, M.; Lanova, B.; Baltruschat, H. Cyclic Voltammetry, FTIRS, and  
49 DEMS Study of the Electrooxidation of Carbon Monoxide, Formic Acid, and Methanol on  
50 Cyanide-Modified Pt(111) Electrodes. *Langmuir* **2009**, *25*, 6500-6507.
- 51  
52 (14) Cabello, G.; Leiva, E. P. M.; Gutiérrez, C.; Cuesta, A. Non-Covalent Interactions at  
53 Electrochemical Interfaces: One Model Fits All? *Phys. Chem. Chem. Phys.* **2014**, *16*, 14281-  
54 14286.
- 55  
56 (15) Artacho, E.; Anglada, E.; Diéguez, O.; Gale, J. D.; García, A.; Junquera, J.; Martín, R.  
57 M.; Ordejón, P.; Pruneda, J. M.; Sánchez-Portal, D.; Soler, J. M. The SIESTA Method;  
58 Developments and Applicability. *J. Phys. Condens. Matter* **2008**, *20*, 064208.
- 59  
60 (16) Perdew, J. P.; Burke, K.; Ernzerhof, M. Generalized Gradient Approximation Made  
Simple. *Phys. Rev. Lett.* **1996**, *77*, 3865-3868.
- (17) Troullier, N.; Martins, J. L. Efficient Pseudopotentials for Plane-Wave Calculations.  
*Phys. Rev. B* **1991**, *43*, 1993-2006.

- 1  
2  
3  
4  
5  
6  
7  
8  
9  
10  
11  
12  
13  
14  
15  
16  
17  
18  
19  
20  
21  
22  
23  
24  
25  
26  
27  
28  
29  
30  
31  
32  
33  
34  
35  
36  
37  
38  
39  
40  
41  
42  
43  
44  
45  
46  
47  
48  
49  
50  
51  
52  
53  
54  
55  
56  
57  
58  
59  
60
- (18) Troullier, N.; Martins, J. L. Efficient Pseudopotentials for Plane-Wave Calculations. II. Operators for Fast Iterative Diagonalization. *Phys. Rev. B* **1991**, *43*, 8861-8869.
- (19) Huerta, F. J.; Morallón, E.; Vazquez, J.; Aldaz, A. Voltammetric and Spectroscopic Characterization of Cyanide Adlayers on Pt(h,k,l) in an Acidic Medium. *Surf. Sci.* **1998**, *396*, 400-410.
- (20) Escudero-Escribano, M.; Soldano, G. J.; Quaino, P.; Zoloff Michoff, M. E.; Leiva, E. P. M.; Schmickler, W.; Cuesta, Á. Cyanide-Modified Pt(111): Structure, Stability and Hydrogen Adsorption. *Electrochim. Acta* **2012**, *82*, 524-533.
- (21) Schardt, B. C.; Stickney, J. L.; Stern, D. A.; Frank, D. G.; Katekaru, J. Y.; Rosasco, S. D.; Salaita, G. N.; Soriaga, M. P.; Hubbard, A. T. Surface Coordination Chemistry of Well-Defined Platinum Electrodes: Surface Polyprotic Acidity of Platinum(111)( $2\sqrt{3} \times 2\sqrt{3}$ )R30°-Hydrogen Isocyanide. *Inorg. Chem.* **1985**, *24*, 1419-1421.
- (22) Schmickler, W.; Guidelli, R. The Partial Charge Transfer. *Electrochim. Acta* **2014**, *127*, 489-505.
- (23) Luque, A. M.; Mulder, W. H.; Calvente, J. J.; Cuesta, A.; Andreu, R. Proton Transfer Voltammetry at Electrodes Modified with Acid Thiol Monolayers. *Anal. Chem.* **2012**, *84*, 5778-5786.
- (24) Marković, N. M.; Lucas, C. A.; Rodes, A.; Stamenković, V.; Ross, P. N. Surface Electrochemistry of CO on Pt(111): Anion Effects. *Surf. Sci.* **2002**, *499*, L149-L158.
- (25) Marković, N. M.; Ross Jr, P. N. Surface Science Studies of Model Fuel Cell Electrocatalysts. *Surf. Sci. Rep.* **2002**, *45*, 117-229.
- (26) Spendelow, J. S.; Goodpaster, J. D.; Kenis, P. J. A.; Wieckowski, A. Mechanism of CO Oxidation on Pt(111) in Alkaline Media. *J. Phys. Chem. B* **2006**, *110*, 9545-9555.
- (27) Spendelow, J. S.; Lu, G. Q.; Kenis, P. J. A.; Wieckowski, A. Electrooxidation of Adsorbed CO on Pt(111) and Pt(111)/Ru in Alkaline Media and Comparison with Results from Acidic Media. *J. Electroanal. Chem.* **2004**, *568*, 215-224.
- (28) Katsounaros, I.; Mayrhofer, K. J. J. The Influence of Non-Covalent Interactions on the Hydrogen Peroxide Electrochemistry on Platinum in Alkaline Electrolytes. *Chem. Commun.* **2012**, *48*, 6660-6662.
- (29) Kodama, K.; Morimoto, Y.; Strmcnik, D. S.; Markovic, N. M. The Role of Non-Covalent Interactions on CO Bulk Oxidation on Pt Single Crystal Electrodes in Alkaline Electrolytes. *Electrochim. Acta* **2015**, *152*, 38-43.
- (30) Stoffelsma, C.; Rodriguez, P.; Garcia, G.; Garcia-Araez, N.; Strmcnik, D.; Marković, N. M.; Koper, M. T. M. Promotion of the Oxidation of Carbon Monoxide at Stepped Platinum Single-Crystal Electrodes in Alkaline Media by Lithium and Beryllium Cations. *J. Am. Chem. Soc.* **2010**, *132*, 16127-16133.
- (31) Tymoczko, J.; Colic, V.; Ganassin, A.; Schuhmann, W.; Bandarenka, A. S. Influence of the Alkali Metal Cations on the Activity of Pt(111) towards Model Electrocatalytic Reactions in Acidic Sulfuric Media. *Catal. Today* **2015**, *244*, 86-102.
- (32) Lebedeva, N. P.; Koper, M. T. M.; Feliu, J. M.; van Santen, R. A. The Effect of the Cooling Atmosphere in the Preparation of Flame-Annealed Pt(111) Electrodes on CO Adlayer Oxidation. *Electrochem. Commun.* **2000**, *2*, 487-490.
- (33) van der Vliet, D. F.; Koper, M. T. M. Electrochemistry of Pt (100) in Alkaline Media: A Voltammetric Study. *Surf. Sci.* **2010**, *604*, 1912-1918.

## TOC Graphic

